Quaternary Research 85 (2016) 456–470

Contents lists available at ScienceDirect

Quaternary Research

journal homepage: http://www.journals.elsevier.com/quaternary-research

Luminescence ages for three 'Middle Palaeolithic' sites in the Nihewan Basin, northern China, and their archaeological and palaeoenvironmental implications

Yu-Jie Guo [a, *], Bo Li [a], Jia-Fu Zhang [b], Bao-Yin Yuan [c], Fei Xie [d], Richard Graham Roberts [a]

[a] Centre for Archaeological Science, School of Earth and Environmental Sciences, University of Wollongong, Wollongong, NSW 2522, Australia
[b] MOE Laboratory for Earth Surface Processes, Department of Geography, College of Urban and Environmental Sciences, Peking University, Beijing 100871, China
[c] Institute of Geology and Geophysics, Chinese Academy of Sciences, Beijing 100029, China
[d] Cultural Relics of Hebei Province, Shijiazhuang 050000, China

ARTICLE INFO

Article history:
Received 22 October 2015
Available online 10 April 2016

Keywords:
Optical dating
K-feldspar
MET-pIRIR
Standardised growth curves
Middle Palaeolithic
Nihewan palaeo-lake
Sanggan River

ABSTRACT

The Nihewan Basin is a key region for studying the Palaeolithic archaeology of East Asia. However, because of the lack of suitable dating methods and representative lithic technologies in this region, the 'Middle Palaeolithic' sites in this basin have been designated based mainly on stratigraphic correlation, which may be unreliable. In this study, three Palaeolithic sites, Motianling, Queergou and Banjingzi, which have been assigned previously to the 'Middle Palaeolithic', are dated based on luminescence dating of K-feldspar grains. Our results show that the cultural layers at Motianling, Queergou and Banjingzi have ages of 315 ± 13, 268 ± 13 and 86 ± 4 ka (corresponding to Marine Isotope Stages 9, 8 and 5), respectively, suggesting that Motianling and Queergou should be assigned to the Lower Palaeolithic, while the age of Banjingzi is consistent with a Middle Palaeolithic attribution. Our results suggest that reassessing the age of 'Middle Palaeolithic' sites in the Nihewan Basin, and elsewhere in North China, is crucial for understanding the presence or absence of the Middle Palaeolithic phase in China. Our dating results also indicate that the Sanggan River developed sometime between about 270 and 86 ka ago.

Introduction

The Chinese 'Middle Palaeolithic'

The division of Palaeolithic stages, especially the 'Middle Palaeolithic', in China and more broadly in East Asia has been hotly disputed since the mid-20th century (e.g., Movius, 1948; Ikawa-Smith, 1978; Gao, 1999; Huang, 2000; Gao and Norton, 2002; Huang et al., 2009; Norton et al., 2009; Yee, 2012). Traditionally, the Chinese Palaeolithic has been divided into three stages: Lower, Middle and Upper Palaeolithic (see reviews in Gao, 1999 and Huang, 2000). However, unlike in western Eurasia, where the Middle Palaeolithic is characterised by distinctive lithic technology (e.g., Levallois prepared cores), the 'Middle Palaeolithic' in China has been defined on the basis of chronology and association with the remains of archaic *Homo sapiens* (Lin, 1996), due mainly to the lack of distinct progress in lithic technology compared to the Lower Palaeolithic (Gao, 1999). In China, sites dated to between the late middle Pleistocene and the middle upper Pleistocene (140–30 ka), and associated with archaic *H. sapiens* remains, have been designated as 'Middle Palaeolithic' (Gao and Norton, 2002). However, the poverty of human remains at Palaeolithic sites in China has resulted in the 140–30 ka interval being the most commonly used criterion to assign archaeological sites to the 'Middle Palaeolithic'. In the past few decades, more than 40 archaeological sites in China have been so assigned, but the ages of most of these sites remain controversial and the most recently obtained ages for some of the sites are much older than proposed originally (see summaries in Gao, 1999 and Norton et al., 2009).

Based on the reanalyses of stone artefacts from 'Middle Palaeolithic' sites in China using four criteria – raw material procurement, core reduction, retouch and typology in stone artefact technology – Gao and colleagues (Gao, 1999; Gao and Norton, 2002; Li, 2014) suggested that the 'Middle Palaeolithic' term should be abandoned in China and proposed, instead, a two-stage

* Corresponding author.
E-mail addresses: yjguo87@gmail.com, yg991@uowmail.edu.au (Y.-J. Guo).

http://dx.doi.org/10.1016/j.yqres.2016.03.002
0033-5894/

model of the Early and Late Palaeolithic. In the latter, the transition from Early Palaeolithic to Late Palaeolithic is defined by the emergence of blade and microblade technologies (Gao and Norton, 2002). This definition is the same as that used to mark the transition from the Middle Palaeolithic to the Upper Palaeolithic in the three-stage model. The two-stage model has been questioned by some other archaeologists (e.g., Huang, 2000; Huang et al., 2009; Yee, 2012). Yee (2012), for example, reassessed the four criteria described above and concluded that stone artefact technology in the Middle Palaeolithic phase shows a gradual transition between the Lower and Upper Palaeolithic phases. In addition, Yee (2012) argued that the two-stage model assumes that changes in human behaviour must occur rapidly, which ignores variability across time and space in the real world (Kleindienst, 2006; Monnier, 2006).

The Nihewan Basin

The Nihewan Basin is an ideal region for studying the palaeoenvironments, palaeontology and Palaeolithic archaeology of East Asia, because of the relatively continuous deposition of fluvio-lacustrine sediments and the abundance of mammalian fossils and stone artefacts found within them (e.g., Zhu et al., 2001, 2004; Ao et al., 2010a,b; Tong, 2012). The basin is located at the north-eastern edge of the Chinese Loess Plateau, ~150 km west of Beijing, in Hebei and Shanxi Provinces (Fig. 1a). It is a fault-formed Cenozoic basin (Yuan et al., 2011), which has at times been covered by a large palaeo-lake (the so-called 'Nihewan palaeo-lake') resulting in fluvio-lacustrine sedimentary deposits (the so-called 'Nihewan Formation') over 100 m thick (Yuan et al., 1996; Zhu et al., 2007). Today, the Nihewan palaeo-lake has disappeared and the Sanggan River runs through the basin from west to east (Fig. 1b). Its tributary, the Huliu River, runs from south to north in the eastern part of this basin (Fig. 1c). Abundant gullies developed along both banks of the Sanggan River during and after the demise of the Nihewan palaeo-lake, creating abundant outcrops of fluvial, lacustrine and overlying loess sediments. The Nihewan Formation does not include the later fluvial deposits of the Sanggan River and its tributaries (Xie et al., 2006; Yuan et al., 2011).

More than 100 Palaeolithic sites have been discovered in this basin (Xie et al., 2006). The Palaeolithic artefacts found in this region are characterised by the 'small tool' industry that may reflect the poor quality of the local raw material, and which spans the time period from early to late Pleistocene (Xie et al., 2006). It has been suggested that no distinct progress in stone artefact technology in this basin occurred before the emergence of micro-blade technologies around ~29 ka ago (Nian et al., 2014). Consequently, like other sites in China, the time interval of 140–30 ka has been used to subdivide Palaeolithic periods in the Nihewan Basin (Xie et al., 2006). However, most of these Palaeolithic sites, and especially those ascribed to the 'Middle Palaeolithic', have not been dated in detail. This is due mainly to the lack of suitable dating methods and the lack of a sound chronological framework for the Nihewan Formation, and for the middle Pleistocene sediments in particular. Consequently, most of these sites have been broadly assigned to the Lower, Middle or Upper Palaeolithic phases based solely on stratigraphic correlations or comparisons of stone artefact technology (Xie et al., 2006). Such approaches may be unreliable and can potentially result in misunderstanding how lithic technologies associated with the small tool industry have developed through time in the basin.

Optical dating

Optical dating can be applied to sediments deposited within and beyond the age range (~50 ka) of radiocarbon (^{14}C) dating and, hence, it provides a suitable means of constructing chronologies for 'Middle Palaeolithic' sites in the Nihewan Basin (Guo et al., 2015). Optical dating has been widely applied to estimate the depositional age of Quaternary sediments around the world (Aitken, 1998; Lian and Roberts, 2006; Wintle, 2014; Roberts et al., 2015) since the technique was first proposed more than 30 years ago (Huntley et al., 1985; Roberts and Lian, 2015). It is used to determine the time elapsed since crystals of minerals such as quartz and potassium-rich feldspar (K-feldspar) were last exposed to sunlight. Quartz is commonly used to date sediments younger than ~200 ka, while K-feldspars can be used to date much older sediments, as the infrared stimulated luminescence (IRSL) signals from K-feldspars saturate at a much higher radiation dose than does the conventional optically stimulated luminescence (OSL) signal from quartz (Roberts et al., 2015). However, the 'anomalous fading' (Wintle, 1973) of luminescence signals in K-feldspars can lead to age underestimation, unless appropriate corrections are made (Huntley and Lamothe, 2001) or fading is greatly reduced or avoided altogether by isolating suitable signals (Li et al., 2014b). A fading-correction method based on laboratory measurements of the fading rate (g-value) is typically only applicable to feldspars younger than ~50 ka (Huntley and Lamothe, 2001). As a result, procedures have been developed recently that decrease or avoid the fading in IRSL signals, including a two-step post-IR IRSL (pIRIR) procedure (Thomsen et al., 2008; Buylaert et al., 2009) and a multiple elevated temperatures (MET) pIRIR (MET-pIRIR) procedure (Li and Li, 2011, 2012). The MET-pIRIR dating procedure and the newly developed pre-dose MET-pIRIR (pMET-pIRIR) procedure (Li et al., 2013, 2014a) can successfully isolate non-fading IRSL signals in feldspars and extend the dating range of the method to the early middle Pleistocene or possibly the late early Pleistocene (e.g., Gong et al., 2014; Li et al., 2014a; Chen et al., 2015; Guo et al., 2015; Meng et al., 2015). Guo et al. (2015) tested pMET-pIRIR procedures on deposits in the Nihewan Basin, and found that sediments with ages of up to ~500 ka (and perhaps as old as 650 ka) could be dated reliably.

In this study, we applied these optical dating procedures to three representative 'Middle Palaeolithic' sites in the Nihewan Basin: Motianling, Queergou and Banjingzi (Figs. 1–4, respectively). The Motianling and Queergou sites have been tentatively attributed to the Middle Palaeolithic based on stratigraphic correlations (Xie et al., 1996, 2006), while the Banjingzi site was so assigned based on U-series ages of about 74–108 ka for a horse tooth recovered from this site (Li et al., 1991; Xie et al., 2006). The lithic technologies at these three sites belong to the small tool industry of the Nihewan Basin. However, the stone artefacts from Motianling and Queergou are claimed to be relatively simple and 'primitive', similar to those found at Lower Palaeolithic sites in the basin, while those from Banjingzi are claimed to be relatively 'advanced' (Xie et al., 2006). These perceived differences in lithic development for three 'Middle Palaeolithic' sites in a small region highlight the need to reassess the chronology of these two distinctive small tool technologies. To determine if they were contemporaneous or not, we have dated the sediments containing the stone tools using single-aliquot regenerative-dose (SAR) pMET-pIRIR procedures for multi-grain single aliquots of K-feldspar and SAR MET-pIRIR procedures for individual K-feldspar grains (Li and Li, 2011; Li et al., 2014a).

Palaeolithic setting

The Motianling site was discovered in 1992 and a total area of 53 m^2, including Localities 1 and 2, was excavated in 2002 (Fig. 2a,b) (Xie et al., 2006). The stone artefacts recovered from the two Localities included cores (n = 6), flakes (n = 10), other tools (n = 20), and several 'chunks' and flaking debris. Four of the stone

https://doi.org/10.1016/j.yqres.2016.03.002 Published online by Cambridge University Press

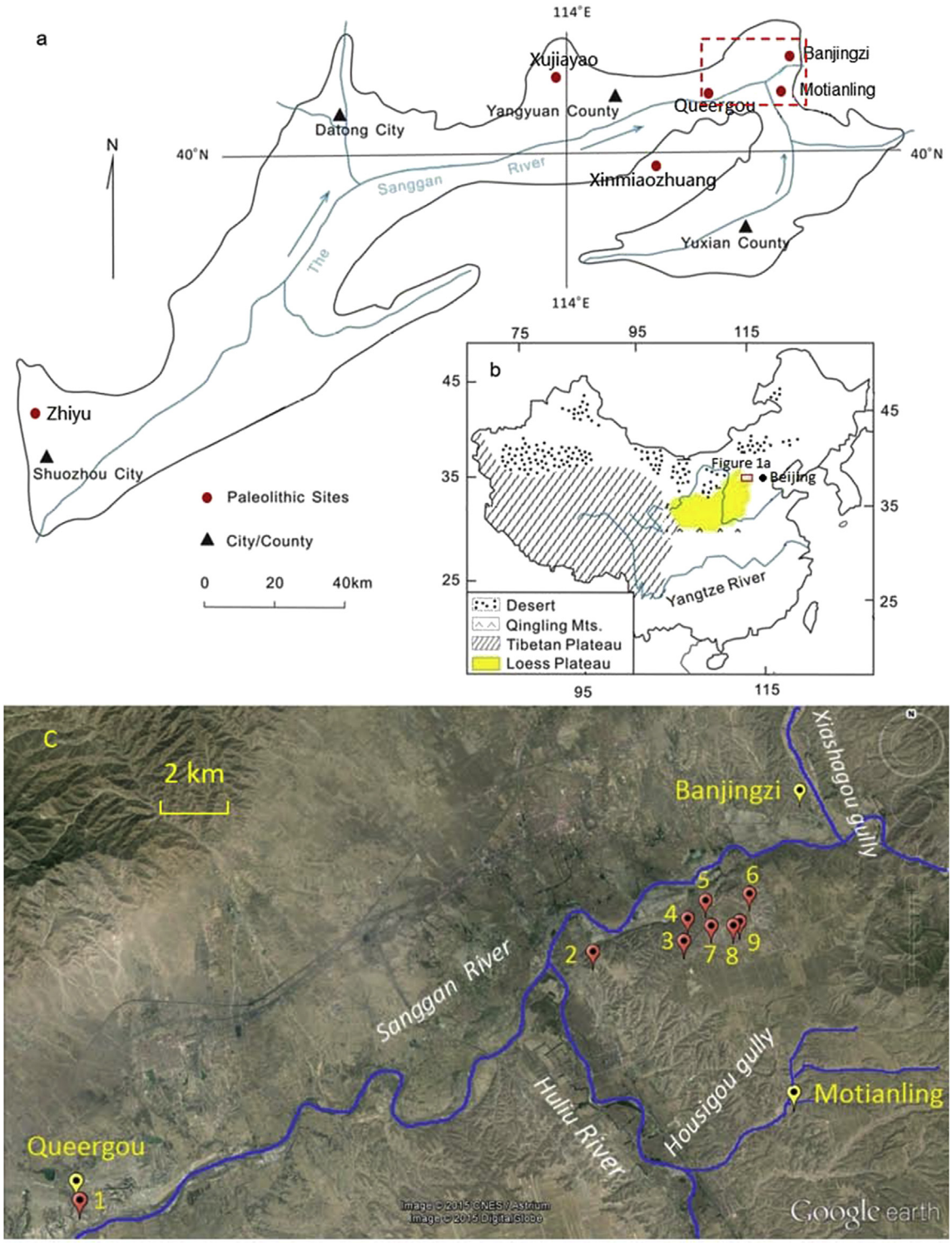

Figure 1. (a) Map of the Nihewan Basin showing the locations of the Motianling, Queergou and Banjingzi Palaeolithic sites (red dashed rectangle); the Xujiayao and Zhiyu sites mentioned in the paper are also marked. (b) Location of the Nihewan Basin (red rectangle) at the northeastern edge of the Loess Plateau (modified from Ao et al., 2010a). (c) Satellite image (courtesy of Google Earth) of the eastern part of the Nihewan Basin (red dashed rectangle in (a)), showing the locations of Motianling, Queergou and Banjingzi (yellow balloons). The Sanggan River, its tributary (the Huliu River), and Xiashagou and Housigou gullies are shown in blue. Other sites mentioned in the text are marked by red balloons: 1. Hutouliang, 2. Haojiatai, 3. Xiaochangliang, 4. Majuangou, 5. Cenjiawan, 6. Youfang, 7. Donggutuo, 8. Maliang and 9. Hougou. (For interpretation of the references to colour in this figure legend, the reader is referred to the web version of this article.)

artefacts excavated from this site are shown in Figure 5. The tool assemblage is simple, including scrapers (n = 11), notches (n = 4), hammers (n = 4) and a chopper (n = 1); the blanks for scrapers and notches are flakes and the flaking method used was hammering. The raw materials mainly comprise flint (56%), siliceous limestone (14%), and quartz sandstone (14%) (Xie et al., 2006). The typologies and manufacturing techniques of the stone artefacts recovered from Motianling are relatively simple, unitary and primitive

https://doi.org/10.1016/j.yqres.2016.03.002 Published online by Cambridge University Press

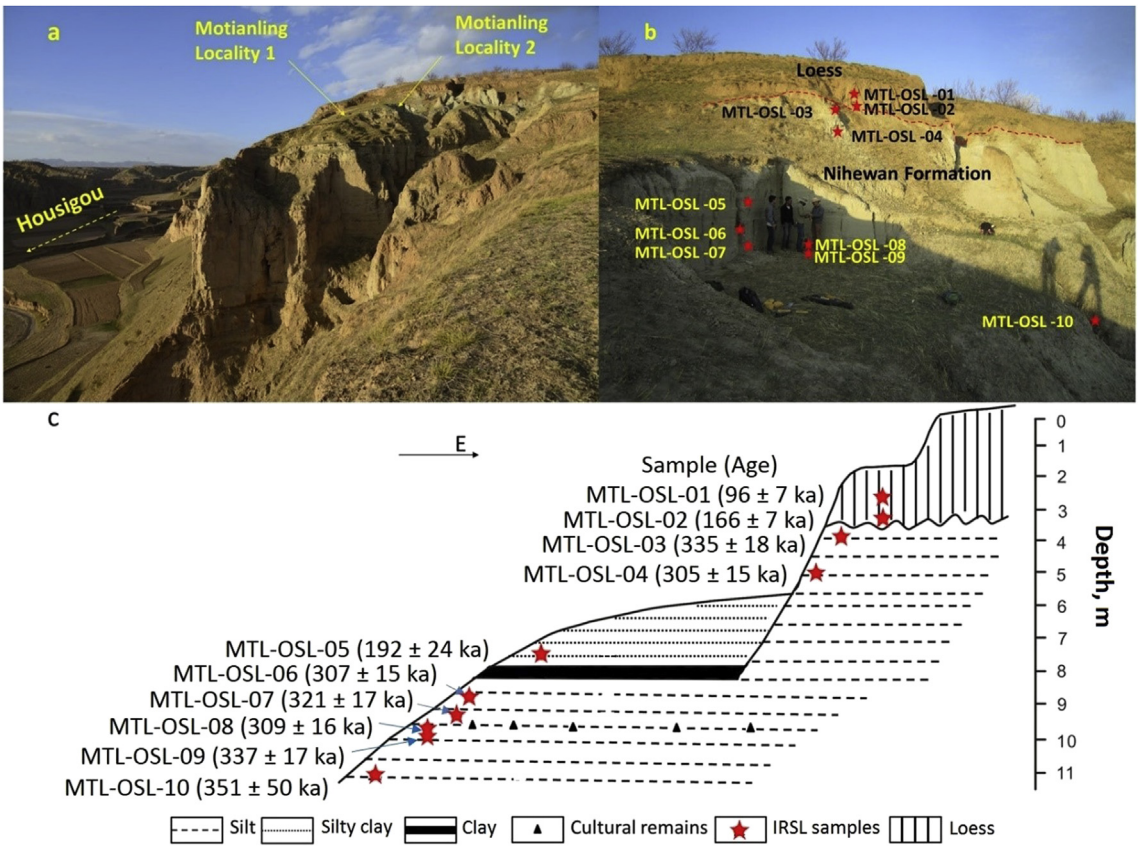

Figure 2. (a) Photo showing the Motianling Palaeolithic site (Localities 1 and 2) and Housigou gully. (b) and (c), Sedimentary profile and sample locations at Locality 2; (c) also shows sample ages.

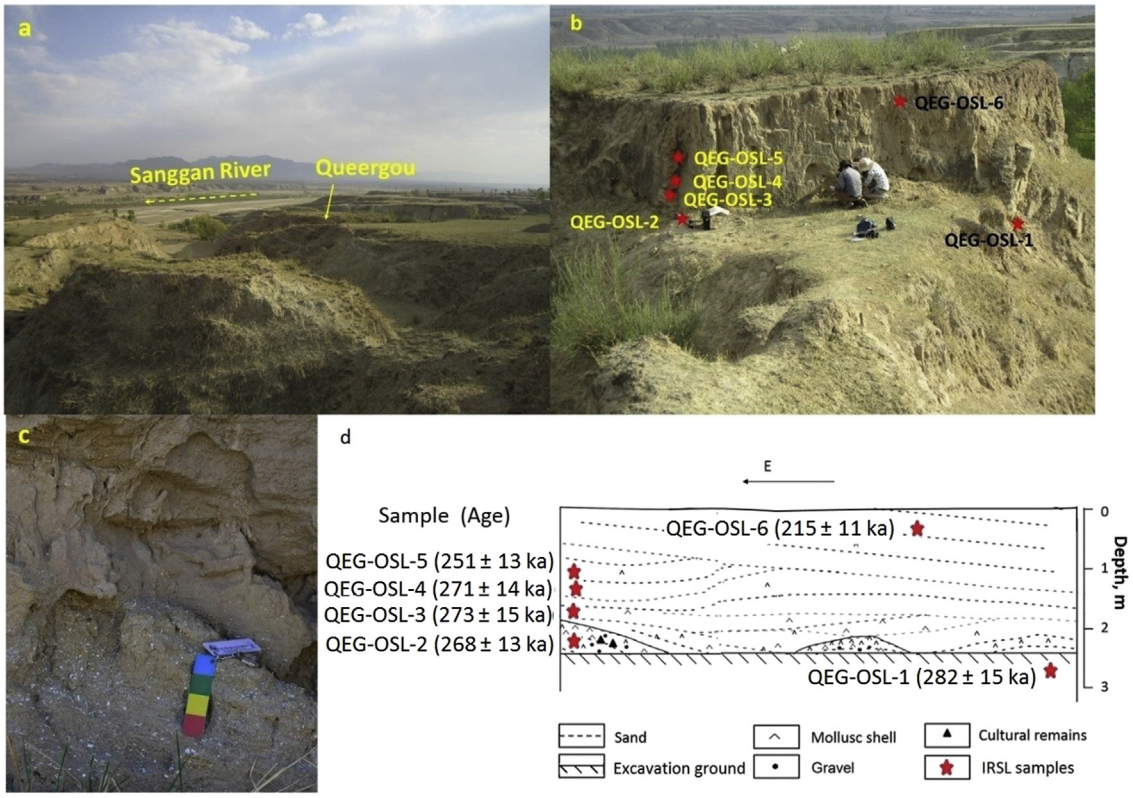

Figure 3. Photos showing (a) the Queergou Palaeolithic site and the Sanggan River, (b) the sample locations at Queergou, and (c) the sands containing mollusc shell fragments. (d) Sedimentary profile and sample locations and ages.

https://doi.org/10.1016/j.yqres.2016.03.002 Published online by Cambridge University Press

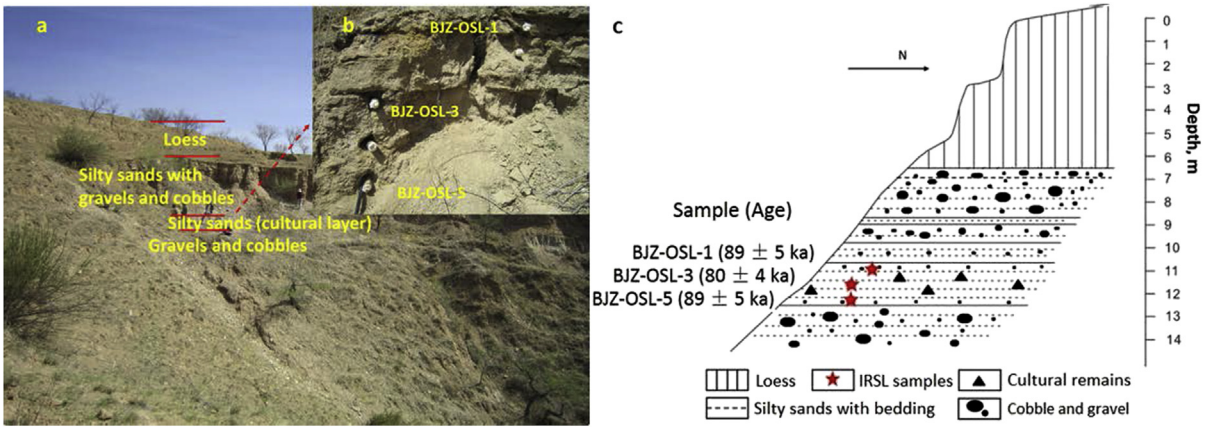

Figure 4. Photos showing (a) the Banjingzi Palaeolithic site, (b) the sample locations at Banjingzi, and (c) sedimentary profile and sample locations and ages.

compared to those from other 'Middle Palaeolithic' sites in the Nihewan Basin (e.g., Xujiayao, Banjingzi and Xinmiaozhuang) (Xie et al., 2006). A total of 146 animal fragments were also recovered and anthropogenic percussion marks were identified on one animal limb bone. *Coelodonta antiquitatis*, *Equus przewalskyi* and *Cervidae gen.et sp.indet* (i.e., Woolly rhinoceros, Przewalski's horse and deer) were identified from these fossils. The cultural remains were considered to be buried in situ, owing to their good state of preservation, and the site was considered as an artefact manufacturing or butchery site (Xie et al., 2006).

The Queergou site was found in 1990, and a total area of 16 m^2 was excavated in 1995 (Xie et al., 1996). A total of 40 stone artefacts and 76 animal fossils have been collected from this site (Xie et al., 1996). The stone artefacts are made from tuff (~45%), quartz (~30%), quartzite, flint, siliceous limestone and quartz sandstone (Xie et al., 1996). The raw materials are available in the nearby area, suggesting that the stone artefacts were made from local materials (Du, 2003). The stone artefacts include cores (n = 5), flakes (n = 6), crude scrapers (n = 3), debris (n = 12) and 'chunks' (n = 14) (Xie et al., 1996). Two stone artefacts excavated from this site are shown in Figure 6. The stone artefacts are similar in their simplicity to those found at the early Pleistocene sites of Majuangou, Xiaochangling, Donggutuo and Cenjiawan (Fig. 1c) in the eastern part of the Nihewan Basin (Xie et al., 2006). *Strothio* sp., *Myospalax fontanieri*, *Cervus* sp., *Equus* sp. and *Rhinoceros* sp. (i.e., Ostrich, Chinese Zokor, deer, horse and rhinoceros) were identified from bone fragments, and anthropogenic percussion marks were identified on one bone fragment (Xie et al., 1996). The cultural remains at this site are thought by some to have been exposed on the ground surface for a long period before being transported to the site by water

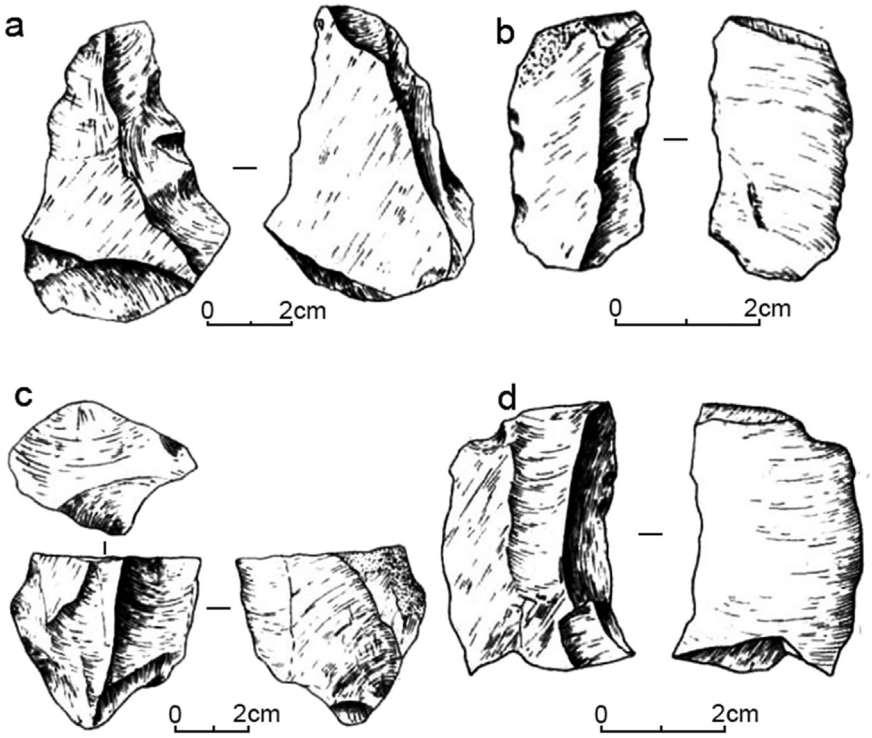

Figure 5. Drawings of stone artefacts at Motianling (from Xie et al., 2006): (a) single-edged scraper (no. 2002MTL Ⅰ: 46), (b) double-edged scraper (no. 2002MTL Ⅱ: 17), (c) core (no. 2002MTL Ⅰ: 43), and (d) notch (no. 2002MTL Ⅱ: 2).

https://doi.org/10.1016/j.yqres.2016.03.002 Published online by Cambridge University Press

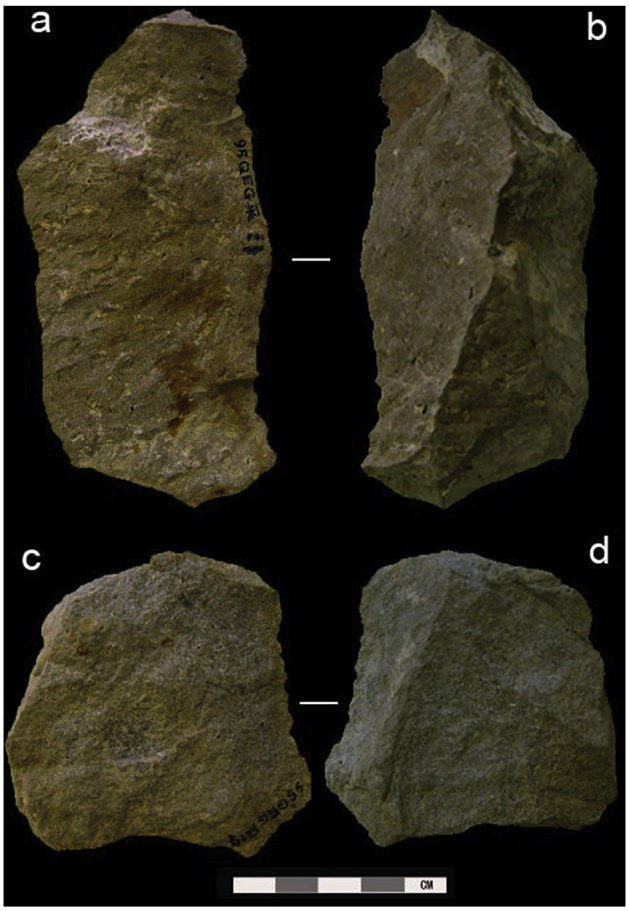

Figure 6. Typical stone artefacts from Queergou: flake no. 1 (a) fracture face and (b) back face, and flake no. 9 (c) fracture face and (d) back face.

flows, owing to traces of physical and chemical weathering on the stone artefacts and animal bones (Xie et al., 1996). However, Yuan et al. (2011) regarded the abundant mollusc fossils in the artefact-bearing layer as evidence that the water flows were shallow and gentle; in addition, the cultural remains recovered from the sands and gravels lens are poorly sorted, indicating that the cultural remains were not transported far by water. The cultural and fossil remains can, thus, be considered to have been buried not far from their original place of deposition. The IRSL ages for the artefact-bearing sediments in this study may, therefore, be contemporaneous with artefact deposition, but younger than the age of manufacture of the artefacts if they have been reworked from the original deposit.

The Banjingzi site was discovered in 1984 and has been excavated five times between then and 1991 (Xie et al., 2006). Stone artefacts recovered in 1988 consist of 215 cores, 1557 flakes, 22 hammers, 329 other tools, 1260 'chunks' and thousands of debris (Li et al., 1991). The tool assemblage is dominated by scrapers (n = 279), points (n = 16), notches (n = 15), end-scrapers (n = 11), choppers (n = 6) and awls (n = 2); the blanks of tools are mainly flakes. The flaking method used was hammering and raw materials are dominated by flint. Based on field investigations, Du (2003) inferred that the raw material was sourced from the Huoshigou area, near the site of Youfang site ~5–6 km away (Fig. 1c), and was processed there before being taken to Banjingzi. The lithic technology at this site is considered to be more 'advanced' than those at Motianling or Queergou, with several prepared cores (Fig. 7e), similar to those produced using the Levallois-Mousterian technique, recovered during excavation (Xie et al., 2006). Figure 7 shows a selection of stone artefacts from this site. Abundant animal fossils were also recovered from the Banjingzi deposits, but bone tools are rare. *Canidae gen.et sp.indet*., *E. przewalskyi*, *C. antiquitatis*, *Cervidae gen.et sp.indet*., *Cervus canadensis*, *Spirocerus* sp., and *Bovinae gen.et sp.indet*. (i.e., dog, Przewalski's horse, Woolly rhinoceros, deer, Canadian red deer, topis and cattle) were identified from the animal fossils. Banjingzi is the only known Middle Palaeolithic site in the Nihewan Basin with evidence of fire use, including a hearth (~40 cm in diameter) containing pieces of charcoal (<1 cm in diameter) and stone artefacts surrounding it (Xie et al., 2006). It is indicated that it might have been a manufacturing site according to the abundance of debris, debitage and 'chunks' (Xie et al., 1996). The preservation and composition of the animal fossils, and the thickness of the cultural layer, suggest that the site was occupied for a lengthy period (Xie et al., 2006). Based on the state of preservation of the stone artefacts and faunal remains, and their spatial distribution, Xie et al. (2006) concluded that the deposits are in situ.

The lithic technologies of the three sites belong to the small tool industry, which has existed in the Nihewan Basin since the early Pleistocene (Xie et al., 2006; Liu et al., 2013). In the basin, the small tool industry is generally thought to have developed continuously (Liu et al., 2013). As mentioned above, however, the lithic technologies at Motianling and Queergou are claimed to be similar (i.e., relatively simple and 'primitive') to those found at Lower Palaeolithic sites in the Nihewan Basin, but distinctly different to the more 'advanced' stone artefacts at Banjingzi (Xie et al., 2006). A straightforward explanation for this is that the development of the small tool industry in the basin may not have been continuous, so the relatively 'advanced' technology at Banjingzi, for example, might have co-existed for only a short period with the simpler technology used since the early Pleistocene. An alternative explanation is that these sites have been ascribed to the same time period incorrectly, due to the lack of a reliable chronology. In particular, an older site incorrectly assigned to a younger period may lead to the erroneous conclusion that there was no development in technology over time. To solve this problem requires that a reliable geochronological framework be established for different Palaeolithic sites. This is especially important for the Nihewan Basin, given the large number of Palaeolithic sites and the long duration of the small tool industry.

Stratigraphic and sample descriptions

The Motianling site (40°10′59″N, 114°41′30″E; 946 m asl) is located at the northeastern edge of the Nihewan Basin (Fig. 1b). It is situated on the south bank of the Housigou gully, a tributary of the Huliu River (Fig. 1c). The site consists of two localities (Localities 1 and 2, Fig. 2a). The sediments at the two localities are both composed of loess, silty clay and silt layers (Fig. 2c). Based on our field investigations, we think that this section might be a terrace of the Housigou gully and the base of the terrace is the Nihewan Formation. In the excavated profile, the lower lacustrine silt layer and the upper fluvial silty clay layer are separated by an impermeable clay layer, ~30 cm thick (Fig. 2c), which marks the boundary between the lower Nihewan Formation and the upper fluvial sediments of the Housigou gully. The thickness of the loess layer at this site is ~3.5 m, while the fluvial silty clay layer ranges from about 1 m to 3 m in thickness. The outcrop of the Nihewan Formation extends to the bed of the modern Housigou gully. Horizontal bedding was observed in the lower clay and silt layers. Cultural remains were excavated from a silt layer (<50 cm thick) in the Nihewan Formation (Fig. 2c). This site has been tentatively assigned to the late Pleistocene by the excavators, based on stratigraphic correlation to

https://doi.org/10.1016/j.yqres.2016.03.002 Published online by Cambridge University Press

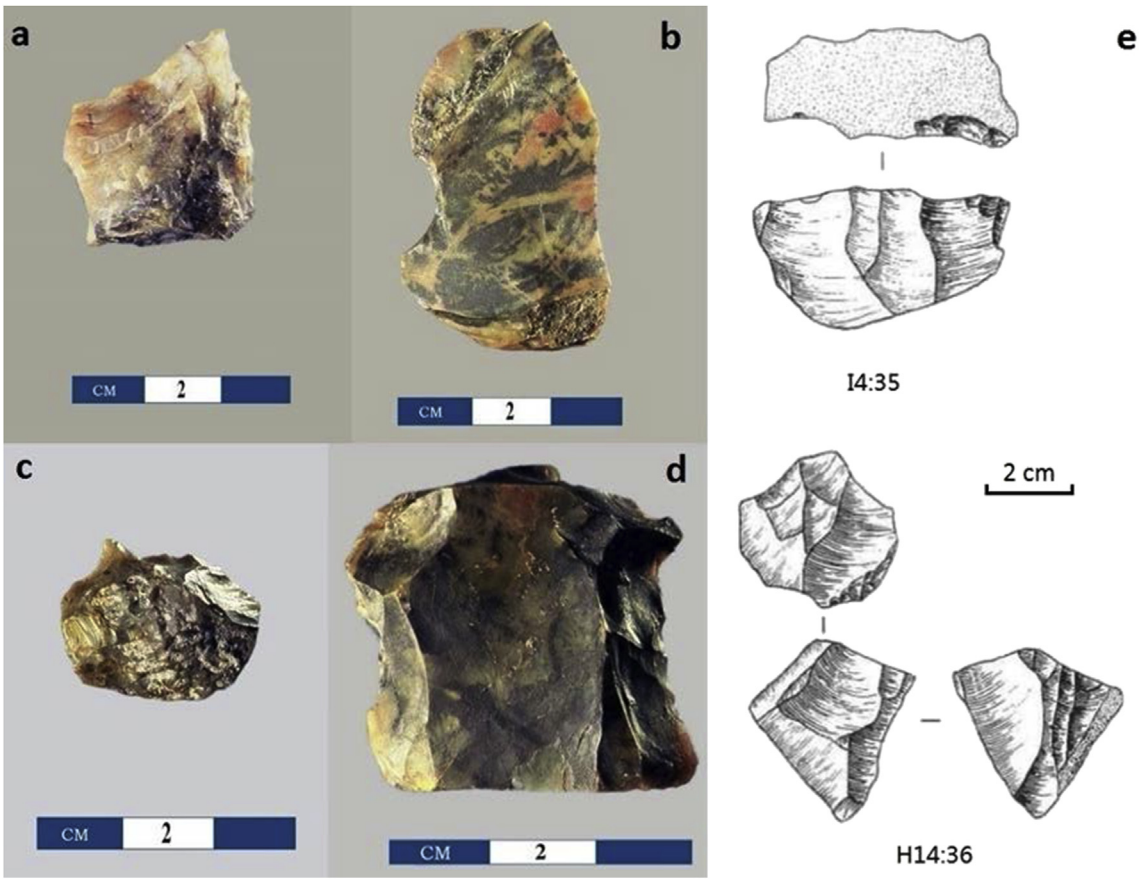

Figure 7. Typical stone artefacts from Banjingzi: (a) notch, (b) scraper, (c) awl, (d) point and (e) cores. Sketch map of (e) was modified after Li et al. (1991). The two cores, numbered as I4:35 and H14:36, were originally described as "funnel-shaped" cores by Li et al. (1991); and the core, numbered as I4:35, was described as "similar to Levallois-Mousterian technique" by Xie et al. (2006).

the Hutouliang and Xishuidi sections (Xie et al., 2006). However, one sample from the cultural layer at this site was previously dated to ~320 ka by us using luminescence methods (Guo et al., 2015). In the present study, 10 samples (MTL-OSL-01 to -10) were collected from the exposed section at Locality 2 (Fig. 2b and c). This includes two samples from the loess layer (MTL-OSL-01 and -02), two from the upper part of the Nihewan Formation (MTL-OSL-03 and -04), one from the fluvial silty clay layer (MTL-OSL-05), and five from the lower Nihewan Formation (MTL-OSL-06 to -10). Samples MTL-OSL-07 and -08 were collected from the top and bottom of the cultural layer, respectively. The dating results of samples MTL-OSL-01, -07 and -10 have been reported (Guo et al., 2015), so only the results for the other seven samples are presented here.

The Queergou site (40°09′56″N, 114°28′45″E; 889 m asl) is located on the north bank of the Sanggan River, about 300 m from the modern Sanggan River (Figs. 1b,c and 3a). The sediments in the excavated profile consist of fluvial sands with oblique bedding in the upper part and cross-bedding in the lower part (Fig. 3d). Cultural remains were recovered from the lens composed of sands and gravels (~0.2–1 cm in diameter) at the base of the excavation. The artefact-bearing layer varies in thickness (but is usually less than ~30 cm thick) and contains abundant mollusc shell fragments (Fig. 3c,d). From this, we infer that the artefact-bearing sediments are lakeshore deposits associated with the Nihewan palaeo-lake. This site was first reported to belong to the upper part of the Nihewan Formation (Xie et al., 1996), based on stratigraphic correlations with two stromatolite layers in the upper part of the Nihewan Formation at the nearby Hutouliang site (Fig. 1c). The stromatolites from the Hutouliang site were dated to about 90 and 130 ka using U-series and ESR dating methods, respectively (Yang et al., 1993). They were subsequently re-analysed using U-series techniques, from it was deduced that U-series and probably also ESR dating are not applicable to the stromatolite, due to their cryptocrystalline structure and the open-system geochemical behaviour of the aragonite (Han et al., 2005). The ages of the two stromatolite layers were re-dated to about 73 and 274 ka by comparing the lightness (L*) of the strata at Hutouliang with the aeolian flux record in the North Pacific Ocean. These age estimates are consistent with the pollen composition of the samples collected from this site (Xia and Han, 1998; Han et al., 2005). A fossil rhinoceros rib from Queergou yielded a U-series age of ~200 ka, but this estimate is also compromised by the open-system behaviour of bone. Other late early Pleistocene (Yuan et al., 2011) or early middle Pleistocene (Xie et al., 2006) age estimates for Queergou have been based on stratigraphic correlations to the sites of Cenjiawan (~1.1 Ma; Wang et al., 2006) or Maliang (~0.79 Ma; Ao et al., 2010b) (Fig. 1c) on the eastern margin of the Nihewan Basin. These ages may be unreliable, however, because they are located ~20 km from Queergou (Xie et al., 2006). Despite the disputed ages for Queergou, archaeologists still tentatively assign this site to the 130–90 ka time interval. To resolve the age of this site, we collected six samples (QEG-OSL-1 to -6) for luminescence dating (Fig. 3b,d). Sample QEG-OSL-2 was collected from the sand and gravel lens (cultural layer) and samples QEG-OSL-OSL-1 and -3 were collected from immediately below and above the lens (Fig. 3b and d), with the remaining three samples collected from the overlying deposits (Fig. 3b,d).

The Banjingzi site (40°15′32″N, 114°42′17″E; 849 asl) is located north of Banjingzi village in Yangyuan County, where the Xiashagou

https://doi.org/10.1016/j.yqres.2016.03.002 Published online by Cambridge University Press

gully meets the Sanggan River (Fig. 1b,c). The deposits are situated on the third terrace (T3) of the Sanggan River (Li et al., 1991). The Nihewan Formation forms the base of the terrace, and the overlying deposits consist of horizontally bedded layers of fluvial silty sand, gravels and cobbles (~0.5–25 cm in diameter) in the lower part and loess in the upper part (Fig. 4c). The latter is ~6.5 m thick, while the outcrops of fluvial deposit are more than 30 m thick (Li et al., 1991). The base of the fluvial deposits has not been exposed at this site, but the boundary between the Nihewan Formation and the overlying terrace deposits is exposed at Banjingzi village (Yuan et al., 2011). Cultural remains were recovered from the upper part of the fluvial sediments. The thickness of the cultural layer was reported as up to ~3 m by Li et al. (1991), but our field investigation exposed only the lower portion (~1.4 m thick) at the margin of the excavation wall; most of the original wall of the excavation trench has since collapsed (Fig. 4a). The age of Banjingzi was estimated to be around 74–108 ka from U-series dating of a horse tooth recovered from the deposits (Li et al., 1991), whereas Wei (1997) estimated the age of the site as ~20 ka, based on geomorphological investigations and stratigraphic correlations with the upper part of the Zhiyu site (Fig. 1a). Given the aforementioned difficulties of dating fossil remains using U-series methods, and the fact that Zhiyu is located at the opposite end of the Nihewan Basin from Banjingzi, we collected five samples (BJZ-OSL-1 to -5) from the outcropping portion of the cultural layer at Banjingzi (Fig. 4b,c) to determine the age of the artefacts. To achieve the latter, three of the 5 samples (BJZ-OSL-1, -3 and -5) were measured, spanning the entire depth interval of the exposed cultural layer.

All the samples in this study were collected in the field by hammering opaque plastic tubes (5 cm in diameter) into the exposed sections or by directly taking blocks of sediments from the cleaned section faces. After the tubes or blocks were removed, they were immediately wrapped in light-proof plastic and transported to the Luminescence Dating Laboratory at the University of Wollongong for analysis. K-feldspar grains of 63–90, 63–106, 90–150 or 180–212 μm in diameter from the samples were extracted following standard mineral separation techniques (Aitken, 1998), and the polymineral fine-grain fraction (4–11 μm in diameter) was prepared following the procedures proposed by Zhang and Zhou (2007) (Table 1). Details about sample preparation methods, measurement facilities and data analysis procedures are given in Supplementary Data.

IRSL and dose rate measurements

The depositional age of the K-feldspar grains is estimated by dividing the equivalent dose (D_e), determined from measurements of the IRSL signal, by the dose rate delivered to those grains (throughout the period of burial) from environmental sources of ionising radiation.

Environmental dose rates

The environmental dose rate for coarse (>63 μm diameter) K-feldspar grains consists of beta, gamma and cosmic radiation contributions external to the grains, plus an internal beta dose rate from the radioactive decay of ^{40}K and ^{87}Rb. The environmental dose rate for fine (4–11 μm in diameter) polymineral grains consists of the external alpha, beta, gamma and cosmic radiation contributions. The beta dose rates for all the samples in this study were estimated using low-level beta counting (Bøtter-Jensen and Mejdahl, 1988) and the procedures described in Jacobs and Roberts (2015). The gamma dose rates for three of our samples (QEG-OSL-2, BJZ-OSL-1 and -5) were measured in the field using in situ gamma-ray spectrometry to account for the inhomogeneity of the sediments within ~30 cm of these samples; the gamma dose rates for the other samples were calculated from laboratory measurements of U and Th activities and K concentrations. The U and Th contents were estimated from thick-source alpha counting (Aitken, 1985) and the K content was measured using X-ray fluorescence (XRF) spectroscopy (see Supplementary Data). For the polymineral sample (MTL-OSL-05), the alpha efficiency (*a*-value) was assumed to be 0.10 ± 0.01 (Kreutzer et al., 2014). The internal dose rate for coarse-grain K-feldspars was estimated by assuming K and Rb concentrations of 13 ± 1% and 400 ± 100 ppm, respectively (Huntley and Baril, 1997; Huntley and Hancock, 2001; Zhao and Li, 2005; Li et al., 2008). The cosmic-ray dose rates were estimated from the burial depth of each of the samples, and the latitude, longitude and altitude of each site (Prescott and Hutton, 1994). The long-term water contents were assumed 10 ± 3% for the loess samples, 15 ± 5% for the fluvial samples and 20 ± 5% for the lacustrine samples (Table 1) in this study (see details in Supplementary Data), which are similar to those used by Zhao et al. (2010) for their samples from the Haojiatai section. Table 1 lists the dosimetry data for our samples.

D_e determinations

Single aliquots

For the Motianling and Queergou samples, we applied the SAR pMET-pIRIR procedure (Li et al., 2014a) to obtain D_e values for the K-feldspar grains. The pMET-pIRIR procedure has been tested previously on samples from Motianling and Donggutuo, and it was found that sediments with ages up to ~500 ka (and possibly 650 ka) could be reliably dated using this procedure (Guo et al., 2015). In the SAR pMET-pIRIR procedure (Supplementary Table 1a), IRSL measurements are performed successively at five temperatures (50, 100, 150, 200 and 250°C) to isolate the non-fading (or least fading) signal at the highest stimulation temperature. A key feature of this procedure is the use of a solar simulator bleach for ~2 h before each of the regenerative doses to 'reset' the dose-dependent sensitivity of the MET-pIRIR signals; this negates the need to correct for sensitivity changes between measurement cycles and, hence, each of the L_x, T_x and L_x/T_x (and L_n, T_n and L_n/T_n) signals can be used to determine D_e values. Typical IRSL decay curves and dose response curves for samples from these two sites are shown in Supplementary Figures 2–5.

To check that the MET-pIRIR signals are satisfactorily bleached by sunlight, a residual dose test was carried out on samples MTL-OSL-02, -03 and -05 and QEG-OSL-2 and -3. The results of these tests are shown in Supplementary Figure 7. The residual dose increases with IR stimulation temperature, as reported in previous studies (Li and Li, 2011; Li et al., 2014b). For these five samples, the residual doses measured at 250°C are 11.5 ± 0.4, 12.0 ± 0.4, 43.7 ± 8.3, 15.7 ± 3.6 and 15.2 ± 2.2 Gy, respectively, which represent about 2.3%, 1.2%, 4.3%, 1.7% and 1.7% of their measured D_e values. Since the residual doses are small compared to the D_e values, we simply subtracted the residual dose from the corresponding D_e estimate for each sample for purposes of age calculation (see Supplementary Data).

Dose recovery tests using the SAR pMET-pIRIR procedure were carried out on samples MTL-OSL-05 and QEG-OSL-2 to validate the applicability of the procedure for samples from these two sites. Two laboratory doses (920 and 800 Gy, respectively) were successfully recovered for the signals measured at 250°C (see Supplementary Fig. 8), suggesting that the SAR pMET-pIRIR procedure can reliably determine D_e values for the samples from Motianling and Queergou under controlled laboratory conditions. We also conducted anomalous fading tests to check that the MET-pIRIR procedure isolates the non-fading signals in our samples; negligible

https://doi.org/10.1016/j.yqres.2016.03.002 Published online by Cambridge University Press

Table 1
Dose rates, D_e values and ages for sediment samples from the Motianling, Queergou and Banjingzi sites.

Sample	Grain size, μm	Water, %	U, ppm	Th, ppm	K, %	Environmental dose rate (Gy/ka)						D_e, Gy[b]	Age, ka
						External[a]				Internal	Total		
						Alpha	Gamma	Beta	Cosmic				
Motianling													
MTL-OSL-01	63–90	10 ± 3	3.43 ± 0.13	7.03 ± 0.98	1.45		0.97 ± 0.06	1.58 ± 0.09	0.17 ± 0.03	0.38 ± 0.03	3.10 ± 0.12	299 ± 20[c] (n = 4, 6)	96 ± 7[d]
MTL-OSL-02	63–90	10 ± 3	3.20 ± 0.13	6.89 ± 1.00	1.36		0.92 ± 0.06	1.45 ± 0.09	0.16 ± 0.03	0.38 ± 0.03	2.91 ± 0.11	483 ± 10 (n = 14)	166 ± 7
MTL-OSL-03	63–90	15 ± 5	3.85 ± 0.14	5.99 ± 1.01	1.48		0.93 ± 0.06	1.54 ± 0.11	0.13 ± 0.03	0.38 ± 0.03	2.98 ± 0.13	997 ± 30 (n = 10)	335 ± 18
MTL-OSL-04	63–90	20 ± 5	7.10 ± 0.21	7.57 ± 1.19	1.49		1.25 ± 0.08	1.72 ± 0.12	0.12 ± 0.03	0.38 ± 0.03	3.47 ± 0.15	1058 ± 28 (n = 10)	305 ± 15
MTL-OSL-05	4–11	20 ± 5	8.96 ± 0.21	7.55 ± 1.00	1.39	1.84 ± 0.34	1.40 ± 0.08	1.83 ± 0.13	0.10 ± 0.03		5.16 ± 0.60	990 ± 38 (n = 12)	192 ± 24
MTL-OSL-06	63–106	20 ± 5	7.41 ± 0.18	3.81 ± 0.73	1.65		1.16 ± 0.07	1.69 ± 0.12	0.09 ± 0.03	0.41 ± 0.03	3.35 ± 0.14	1028 ± 24 (n = 10)	307 ± 15
MTL-OSL-07	63–106	20 ± 5	4.67 ± 0.16	6.17 ± 1.05	1.64		1.00 ± 0.07	1.63 ± 0.11	0.08 ± 0.03	0.41 ± 0.03	3.13 ± 0.14	1004 ± 30 (n = 10)	321 ± 17[d]
MTL-OSL-08	63–106	20 ± 5	3.57 ± 0.14	8.61 ± 1.08	1.71		1.01 ± 0.07	1.61 ± 0.11	0.08 ± 0.03	0.41 ± 0.03	3.12 ± 0.14	963 ± 28 (n = 10)	309 ± 16
MTL-OSL-09	63–90	20 ± 5	4.26 ± 0.14	7.54 ± 1.02	1.64		1.02 ± 0.07	1.53 ± 0.10	0.08 ± 0.03	0.38 ± 0.03	3.01 ± 0.13	1014 ± 24 (n = 10)	337 ± 17
MTL-OSL-10	63–90	20 ± 5	2.76 ± 0.14	9.82 ± 1.22	2.04		1.05 ± 0.07	1.75 ± 0.12	0.07 ± 0.03	0.38 ± 0.03	3.25 ± 0.15	1143 ± 153[c] (n = 4, 4)	351 ± 50[d]
Queergou													
QEG-OSL-01	90–150	15 ± 5	3.67 ± 0.14	7.39 ± 1.01	1.80		1.04 ± 0.07	1.65 ± 0.12	0.16 ± 0.03	0.58 ± 0.04	3.42 ± 0.15	963 ± 33 (n = 20)	282 ± 15
QEG-OSL-02[e]	90–150	15 ± 5					1.00 ± 0.06	1.65 ± 0.11	0.16 ± 0.03	0.58 ± 0.04	3.39 ± 0.14	909 ± 25 (n = 20)	268 ± 13
QEG-OSL-03	90–150	15 ± 5	2.63 ± 0.11	5.61 ± 0.87	1.76		0.86 ± 0.06	1.54 ± 0.11	0.17 ± 0.03	0.58 ± 0.04	3.15 ± 0.13	860 ± 31 (n = 20)	273 ± 15
QEG-OSL-04	90–150	15 ± 5	3.46 ± 0.13	7.50 ± 1.00	1.65		0.99 ± 0.07	1.52 ± 0.11	0.18 ± 0.03	0.58 ± 0.04	3.27 ± 0.14	886 ± 24 (n = 17)	271 ± 14
QEG-OSL-05	90–150	15 ± 5	2.38 ± 0.12	7.50 ± 1.04	1.72		0.90 ± 0.06	1.59 ± 0.11	0.18 ± 0.03	0.58 ± 0.04	3.25 ± 0.14	816 ± 21 (n = 16)	251 ± 13
QEG-OSL-06	90–150	15 ± 5	4.16 ± 0.16	7.38 ± 1.15	1.65		1.05 ± 0.07	1.65 ± 0.12	0.20 ± 0.03	0.58 ± 0.04	3.48 ± 0.15	748 ± 20 (n = 13)	215 ± 11
Banjingzi													
BJZ-OSL 1[e]	180–212	15 ± 5					0.89 ± 0.05	1.68 ± 0.11	0.08 ± 0.03	0.91 ± 0.07	3.56 ± 0.71	316 ± 12 (n = 133)	89 ± 5
BJZ-OSL 3	180–212	15 ± 5	2.38 ± 0.12	7.50 ± 1.04	1.69		0.90 ± 0.06	1.45 ± 0.10	0.08 ± 0.03	0.91 ± 0.07	3.33 ± 0. 74	266 ± 9 (n = 172)	80 ± 4
BJZ-OSL 5[e]	180–212	15 ± 5					0.98 ± 0.06	1.64 ± 0.11	0.07 ± 0.03	0.91 ± 0.07	3.61 ± 0.71	322 ± 10 (n = 199)	89 ± 5

[a] The external gamma, beta and cosmic-ray dose rates have been corrected for water attenuation. The cosmic-ray dose rates were estimated from the burial depth of each sample and the latitude, longitude and altitude of each site, and the final dose rates determined as the mean of the values obtained assuming rapid and steady rates of sample burial to their present depths; these dose rates have been assigned relative errors of ±15% to accommodate uncertainties in their burial history and a possible systematic error in the primary cosmic-ray intensity (Prescott and Hutton, 1994).

[b] For the Motianling and Queergou sites, the D_e value for each sample was calculated as the weighted mean of the single-aliquot D_e values obtained by projecting the L_n signals on to the corresponding SGCs; the over-dispersion values of the single-aliquot D_e distribution of each sample are all less than 14%. Values in parentheses (n) indicate the number of the aliquots used to determine the final D_e values, which were estimated using the central age model. For the Banjingzi samples, the D_e values were estimated for individual grains by projecting the sensitivity-corrected natural signals on to the corresponding dose response curves; the single-grain D_e distributions were then fitted using the finite mixture model and the weighted mean D_e determined for the main component. The D_e values minus the residual doses were used for the final age calculation. The measurement errors on each D_e include photon counting statistics; instrumental irreproducibility errors of 1.5% and 2% for each single-aliquot and single-grain IRSL measurement, respectively; curve fitting errors; and, for single grains, the errors associated with calibrating the beta dose rate delivered to individual grain positions. A systematic error of 2% was also added in quadrature to the D_e measurement errors for possible bias in the calibration of the laboratory beta source.

[c] D_e values reported by Guo et al. (2015) minus the residual dose. The values in parentheses (n) indicate the number of aliquots used to determine the final D_e values using the SAR or MAR method (listed first and second, respectively).

[d] Ages for samples MTL-OSL-01, -07 and -10 are calculated here based on the dose rates measured using low-level beta counting for beta dose rate determination and thick-source alpha counting (U and Th) plus X-ray fluorescence spectroscopy (K) for gamma dose rate determination. In Guo et al. (2015), the ages for these 3 samples were reported as 102 ± 7, 322 ± 33 and 370 ± 50 ka, respectively, based on the dose rates measured using a combination of beta counting and thick-source alpha counting. The ages obtained using these different approaches are consistent at 1σ, but we consider that the ages reported here as more accurate.

[e] The gamma dose rates for samples QEG-OSL-2, BJZ-OSL-1 and -5 were measured using a portable gamma-ray spectrometer, and the beta dose rates were measured by low-level beta counting.

fading rates (*g*-values) of less than 1% per decade (normalised to a delay time of 2 days) were obtained at IR stimulation temperatures of 250°C and higher (Guo et al., 2015; Supplementary Fig. 9).

Based on the performance tests described above, we used the SAR pMET-pIRIR procedure to estimate the D_e values for the Motianling and Queergou samples. Given the large D_e values of our samples, regenerative doses up to 2000 Gy are required to bracket the natural doses, which is time-consuming. To reduce instrument time, we established standardised growth curves (SGCs) for each of these two sites, following the method proposed by Li et al. (2015a,b). Samples MTL-OSL-02, -07 and -09 and QEG-OSL-1, -2 and -6 were measured using a full SAR procedure to construct their

https://doi.org/10.1016/j.yqres.2016.03.002 Published online by Cambridge University Press

dose response curves. For the 250°C L_x/T_x, L_x and T_x signals, the dose response curves were then 're-normalised' (Li et al., 2015a,b) to establish SGCs for each site. The dose response curves for the three samples from each site are indistinguishable (Supplementary Figs. 3 and 4), and the D_e values obtained from the full SAR curves and the SGCs are consistent at 1σ for the same samples (Fig. 8). Based on this finding, D_e values for the other samples (MTL-OSL-03, -04, -06 and -08, and QEG-OSL-3, -4 and -5) were obtained by measuring only their natural signal, one regenerative-dose signal, and the corresponding test dose signals, and then projecting the re-normalised natural IRSL signals on to the L_x/T_x, L_x and T_x SGCs (Supplementary Figs. 3 and 4). For polymineral sample MTL-OSL-05, the D_e values for 12 separate aliquots were measured using the full SAR procedure (Supplementary Fig. 5).

The D_e values obtained from the L_x/T_x, L_x and T_x signals are plotted against the corresponding IR stimulation temperatures for MTL-OSL-05 and QEG-OSL-2 in Supplementary Figure 10. The pattern of D_e values versus stimulation temperature is consistent with the dose recovery test results for these two samples (Supplementary Fig. 8) and with those reported for MTL-OSL-07 in our previous study (Guo et al., 2015), and indicate the existence of non-fading signals at elevated stimulation temperatures. On the basis of these findings, we conclude that D_e values obtained for the 250°C L_x/T_x, L_x and T_x signals accurately reflect the natural doses of the samples from Motianling and Queergou. Given the higher precision and accuracy of the L_x signal and its potential for measuring higher doses, we used the D_e values obtained from the 250°C L_x signals for final age determination of the samples from these two sites (Table 1).

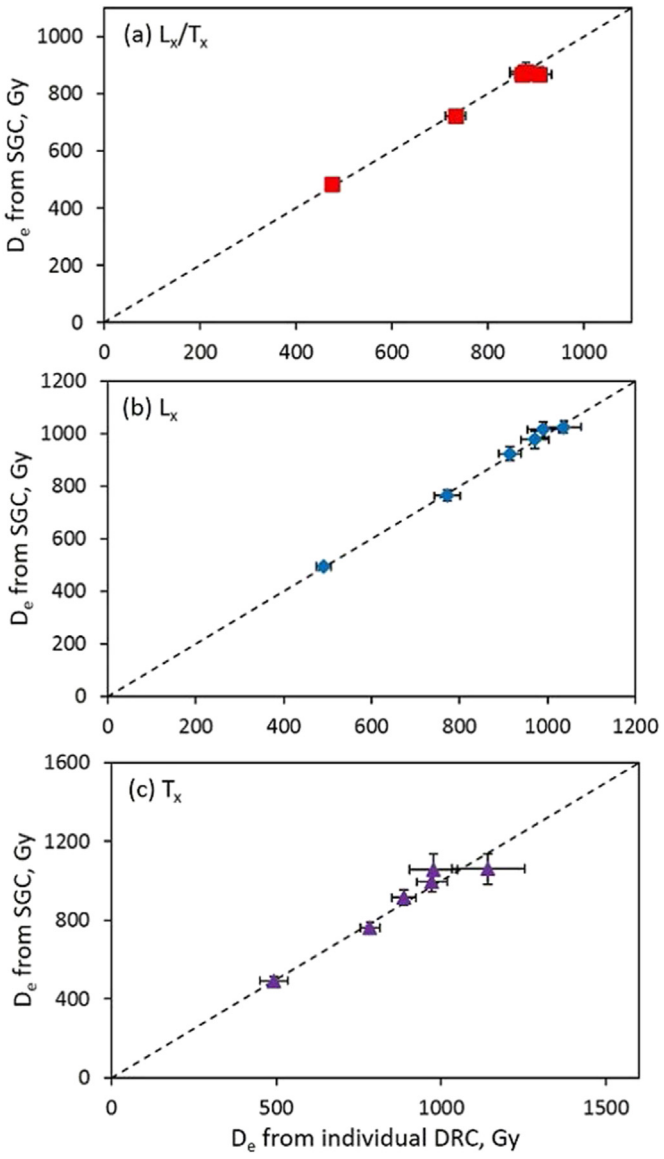

Figure 8. D_e values obtained from individual single-aliquot dose response curves (DRCs) of samples MTL-OSL-02, -07 and -09 and QEG-OSL-1, -2 and -6, plotted against the D_e values obtained from the standardised growth curves (SGCs) for the (a) L_x/T_x, (b) L_x and (c) T_x signals (see Supplementary Figs. 3 and 4).

Single grains

D_e measurements were made on single grains of K-feldspar for the three Banjingzi samples (BJZ-OSL-1, -3 and -5), owing to inhomogeneity of the fluvial sediments around the sampling positions (Fig. 4c). Fluvially transported sediments may be insufficiently bleached before deposition, and at archaeological sites they may also suffer from post-depositional disturbance due to human activities. We used a single-grain MET-pIRIR procedure similar to that proposed by Blegen et al. (2015), which is based on the conventional SAR MET-pIRIR procedure (Li and Li, 2011), except that the 250°C IRSL stimulation using IR diodes is replaced by an IR laser for stimulation of individual grains at this temperature (Supplementary Table 1b). This procedure does not benefit from the solar stimulator bleach used to reset the dose-dependent sensitivity of the MET-pIRIR signals (as used in the pre-dose procedure), so only the sensitivity-corrected signals (L_n/T_n and L_x/T_x) can be used for D_e estimation.

The IRSL signal from a representative grain of sample BJZ-OSL-3 and its corresponding dose response curve are shown in Supplementary Figures 11a and b, respectively. Several criteria have been proposed to reject quartz grains that are ill-suited to single-grain measurements (Jacobs et al., 2006), and these have been adapted to single grains of K-feldspar (Li et al., 2011; Blegen et al., 2015). Further details about the measurement procedures and characteristics of the rejected grains are provided in Supplementary Data and Supplementary Table 2.

To test the suitability of the single-grain MET-pIRIR procedure for sample BJZ-OSL-3, a dose recovery test was performed: a laboratory dose of 310 Gy was given to bleached grains and then measured as the surrogate natural dose. The dose recovery ratios (recovered dose/given dose) for individual grains are displayed in Supplementary Figure 12a. The mean ratio of recovered dose to given dose is 1.00 ± 0.03 after subtracting the residual dose (see below), which is statistically consistent with unity and suggests that the single-grain MET-pIRIR procedure (Supplementary Table 1b) is suitable for dating K-feldspar grains from Banjingzi. A residual dose test was also conducted on single grains from the same sample. All grains, except one with a residual dose of 43 ± 15 Gy, have residual doses consistent with a mean value of 12.4 ± 1.0 Gy (Supplementary Fig. 12b); the latter is reduced insignificantly (to 11.9 ± 0.5 Gy) by omitting the grain with a residual dose of ~43 Gy. A residual dose of 12.4 Gy represents less than 5% of the D_e values for the three samples, so we simply subtracted this amount from the measured D_e of each sample. We also conducted a fading test on single aliquots of sample BJZ-OSL-5, using the same MET-pIRIR procedure as used for sample QEG-OSL-2. Negligible fading rates (g-values) of 0.8 ± 0.3 and −0.6 ± 0.9% per decade were obtained for the L_x/T_x signals measured at 250 and 280°C, respectively (Supplementary Fig. 9b).

Based on the favourable results of these performance tests, the single-grain MET-pIRIR procedure was applied to the Banjingzi samples. A total of 500 K-feldspar grains were measured for each sample, of which D_e values were obtained for 133, 172 and 199 grains of samples BJZ-OSL-1, -3 and -5, respectively. The D_e values

https://doi.org/10.1016/j.yqres.2016.03.002 Published online by Cambridge University Press

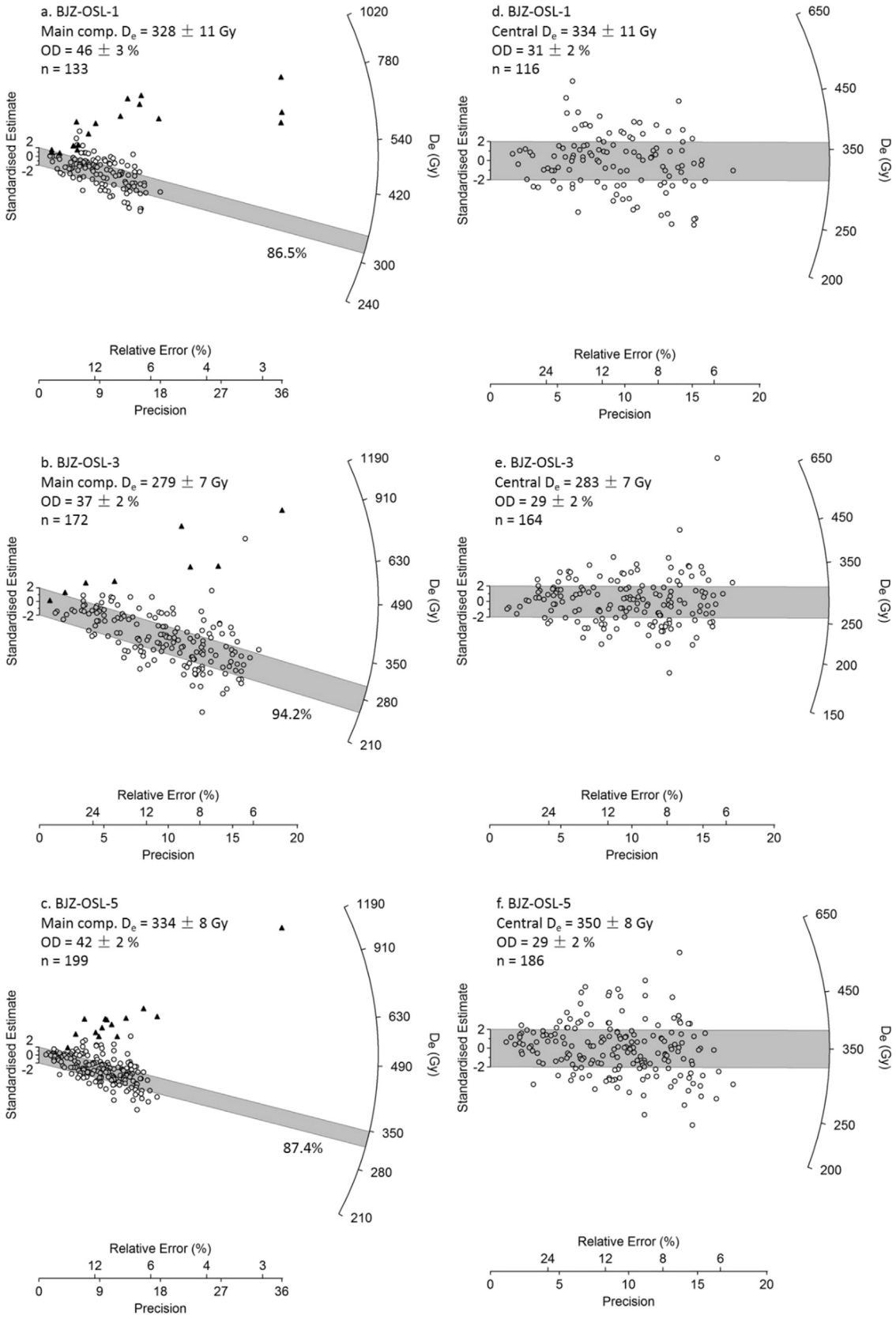

Figure 9. D_e distributions for all accepted K-feldspar grains for samples (a) BJZ-OSL-1, (b) BJZ-OSL-3 and (c) BJZ-OSL-5. The grey band is centred on the weighted mean D_e of the main component fitted using the finite mixture model. The filled triangles denote the few high D_e values that exceed $3D_0$ (see Supplementary Data). (d)–(f), corresponding D_e distributions after excluding D_e values $>3D_0$.

https://doi.org/10.1016/j.yqres.2016.03.002 Published online by Cambridge University Press

for the accepted grains of each sample are displayed in Figure 9. Each of the distributions has a few high D_e values, with the majority of D_e values scattered around a central value of 280–350 Gy. There is no evidence of clustering of D_e values at the leading edge of the distribution, as has been reported for samples containing partially bleached grains (Olley et al., 1999, 2004). To determine the D_e values of the majority of grains in each sample, we applied the finite mixture model (Roberts et al., 2000; Galbraith, 2005) to estimate the D_e values and relative proportions of grains in each of two components (David et al., 2007; Jacobs et al., 2008; Galbraith and Roberts, 2012). One of these components contains most of the grains and the other consists of the few high D_e values. The latter represent D_e values that are close to the saturation level of their individual dose response curves (>3 times the characteristic saturation dose, D_0) and which we consider to be unreliable estimates of D_e. Well-established statistical methods (see Supplementary Data) were used to fit two components to each D_e distribution and determine their weighted mean D_e values and the proportion of grains in each component; Supplementary Table 3 gives a worked example for sample BJZ-OSL-5. The lower (main) D_e component accounts for about 86.5%, 94.2% and 87.4% of the total number of accepted grains for samples BJZ-OSL-1, -3 and -5, respectively. The corresponding weighted mean D_e values of this component (328.4 ± 10.6, 278.7 ± 6.8 and 334.2 ± 7.6 Gy) were used for age determination, after subtracting a residual dose of 12.4 ± 1.0 Gy.

Luminescence chronologies and their regional implications

Palaeoenvironmental conditions in the Nihewan Basin

The sample ages are summarised in Table 1. For the Motianling site, the ages for the samples from the upper part of the stratigraphy (MTL-OSL-01 to -04) and the samples from the lower excavation pit (MTL-OSL-05 to -10) are in broad accord with their stratigraphic position (Fig. 2). The two ages for the cultural layer (samples MTL-OSL-07 and -08) are statistically consistent and the weighted mean value of 315 ± 13 ka obtained using the central age model (Galbraith et al., 1999; Galbraith and Roberts, 2012) is considered the most accurate and precise estimate of the age of the cultural layer. The ages of the two loess samples (96 ± 7 and 166 ± 7 ka) indicate that loess began to accumulate in this area at least ~166 ka ago. The ages of the lacustrine samples (MTL-OSL-03, -04 and -06 to -10) are consistent at 1σ, and give a weighted mean age of 319 ± 10 ka. There is a time gap of ~150 ka between the loess and the underlying lacustrine sediments. This loess-lacustrine sedimentation gap has also been reported for the nearby Haojiatai and Hougou localities (Fig. 1c), where time gaps of around 140 and 290 ka duration were determined using recuperated OSL dating procedures for quartz (Zhao et al., 2010) and pIRIR dating procedures for K-feldspars (Nian et al., 2013), respectively. Sample MTL-OSL-05 was collected from the upper terrace of Housigou gully and has an age of 192 ± 24 ka, which indicates that there was also a gap in sedimentation of ~130 ka between deposition of the Nihewan Formation and the overlying terrace sediments. This indicates that erosion took place during and/or after the retreat of the Nihewan palaeo-lake, with the depth of erosion varying between localities.

For the Queergou site, the sample ages are also consistent with their stratigraphic positions (Fig. 3). The sediments comprising the cultural layer (sample QEG-OSL-2) were deposited 268 ± 13 ka ago, but the cultural remains might be older as they were not buried in situ and may had been exposed for a long period before burial (see earlier discussion). Sample QEG-OSL-2 was collected from the lakeshore sediments of the Nihewan palaeo-lake, so the age of ~270 ka represents the time when the Nihewan palaeo-lake had retreated to Queergou. This age is consistent with the ~274 ka age inferred for the lower stromatolite layer at Hutouliang (Fig. 1c) (Han et al., 2005) and indicates that stromatolites were living in the shallow waters of the Nihewan palaeo-lake (Xia and Han, 1998). The Queergou site is ~50 ka younger than the top of the Nihewan Formation (~320 ka) at Motianling. This time gap may represent the time taken by the Nihewan palaeo-lake to retreat from Motianling area (946 m asl) to Queergou (889 m asl) or it could be due to erosion for a gap in sedimentation at the top of the Nihewan Formation at Motianling, so the rapid retreat of the palaeo-lake cannot be ruled out.

At Banjingzi, the ages of the three samples from the cultural layer (89 ± 5, 80 ± 4 and 89 ± 5 ka) are consistent at 1σ and give a weighted mean age of 86 ± 4 ka. This falls within the U-series age range of 74–108 ka obtained for a horse tooth recovered from this site (Li et al., 1991). The sediment samples were collected from the upper part of the third terrace (T3) of the Sanggan River at Banjingzi (Xie et al., 2006), so the age of ~86 ka should be close to the abandonment age of this terrace.

To explore the regional climatic and environmental conditions in the vicinity of these three sites, and their possible influence on human dispersal and evolution in the region (e.g., Dennell, 2013; Mu et al., 2015), we have compared in Figure 10 the IRSL ages for the three sites to global marine isotope records (Lisiecki and Raymo, 2005) and the magnetic susceptibility (MSUS) loess proxy curve from the Xifeng section in the Chinese Loess Plateau (Guo et al., 2009). The ages of the cultural layers at Motianling (315 ± 13 ka) and Banjingzi (86 ± 4 ka) correspond to the Marine Isotope Stages (MIS) 9 and 5 interglacial periods, and to palaeosol development during MSUS periods S3 and S1, respectively, indicating wet and warm conditions during human occupation of these two sites. The age of the cultural layer at Queergou (268 ± 13 ka) corresponds to the glacial period of MIS 8 and deposition of loess during MSUS period L3, indicating a cold and dry climate. However, as the cultural remains at Queergou may have been redeposited (Xie et al., 1996, 2006), we cannot infer that the site was occupied under cold conditions.

Based on our new ages, we conclude that the Nihewan palaeo-lake had retreated to the Queergou–Hutouliang area ~270 ka ago, perhaps as a result of regional climatic change from warm and wet (MIS 9) to cold and dry (MIS 8) conditions. However, as the top of the lacustrine sediments at Motianling (319 ± 10 ka) may have been eroded, we cannot rule out the rapid retreat of the Nihewan palaeo-lake due to tectonic uplift (Zhu et al., 2007; Yuan et al., 2009). Some combination of tectonic and climatic effects is also possible. The Sanggan River developed sometime between about 270 and 86 ka ago, but more geomorphological and geochronological studies are needed to provide a more complete account of the development of the Sanggan River and the disappearance of the Nihewan palaeo-lake.

Implications for the 'Middle Palaeolithic' of North China

We have reassessed the chronology of three sites (Motianling, Queergou and Banjingzi) in the Nihewan Basin that have been attributed to the 'Middle Palaeolithic' in the traditional three-stage model. The Banjingzi site contains stone artefacts that are claimed to be more technologically 'advanced' than those found at Lower Palaeolithic sites in this basin (Xie et al., 2006), which would appear to favour the three-stage model. Our dating results for Banjingzi indicate that the cultural remains at this site are ~86 ka in age, which supports their previous attribution to the Middle Palaeolithic (Li et al., 1991; Xie et al., 2006). At Motianling and Queergou, however, the stone artefacts are claimed to be relatively simple and differ little from those found at Lower Palaeolithic sites (Xie et al.,

https://doi.org/10.1016/j.yqres.2016.03.002 Published online by Cambridge University Press

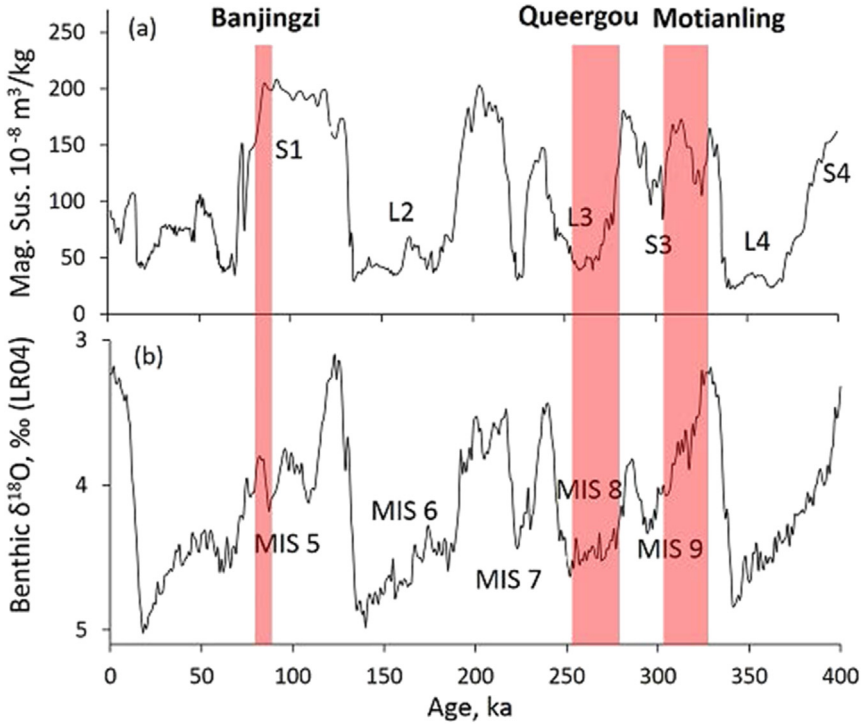

Figure 10. (a) IRSL ages of the upper lacustrine sediments at Motianling (319 ± 10 ka), the lakeshore sediments at Queergou (268 ± 13 ka) and the terrace deposits of the Sanggan River at Banjingzi (86 ± 4 ka), plotted against the magnetic susceptibility (MSUS) loess proxy curve from the Xifeng section (Guo et al., 2009). S1, S3 and S4 correspond to periods of palaeosol development, and L2, L3 and L4 to periods of loess deposition. (b) IRSL ages plotted against the globally distributed oxygen isotope record of marine benthos (Marine Isotope Stages) (Lisiecki and Raymo, 2005).

2006); this would appear to support the alternative, two-stage model that posits a lack of progress in lithic technology from the Lower to the Middle Palaeolithic. Our luminescence ages indicate that the cultural remains at Motianling and Queergou are actually around 310 and 270 ka, respectively (and possibly older at Queergou), rather than 140–30 ka as proposed previously for the Middle Palaeolithic. These two assemblages should therefore be assigned to the Lower Palaeolithic, rather than to the Middle Palaeolithic, if a three-stage model is adopted.

Given the large number of undated or poorly dated 'Middle Palaeolithic' and upper Lower Palaeolithic sites in the Nihewan Basin, and across North China more broadly, further studies are required to establish firm age control throughout the region. We recognise, however, that establishing a reliable chronology for Palaeolithic sites cannot, by itself, resolve the issue of the 'Middle Palaeolithic' in North China: this also requires detailed consideration of the technological and typological characteristics of the artefact assemblages, including methodological issues such as sample size, choice of raw material, and site and artefact function. Additional geoarchaeological information on site formation and post-depositional processes would also be valuable. Through the combination of these insights, the spatio-temporal development and spread of Palaeolithic technologies across North China can be better understood.

Conclusions

Three 'Middle Palaeolithic' sites (Motianling, Queergou and Banjingzi) in the Nihewan Basin of northern China have been dated in this study using newly developed (pre-dose) MET-pIRIR dating procedures for multi-grain aliquots and single grains of K-feldspar. Our results suggest that the cultural layers at Motianling, Queergou and Banjingzi were deposited 315 ± 13 (MIS 9), 268 ± 13 (MIS 8) and 86 ± 4 (MIS 5) ka ago, respectively. Our ages also indicate that the Sanggan River developed sometime between about 270 and 86 ka ago, but further research is needed to reveal the details of the late Quaternary history of the Sanggan River and the Nihewan palaeo-lake.

As the commonly accepted time span for the Chinese 'Middle Palaeolithic' is about 140–30 ka ago, we infer that Motianling and Queergou should be reassigned to the Lower Palaeolithic, whereas the Banjingzi is consistent with a Middle Palaeolithic age. Our luminescence chronologies have helped resolve the conundrum of contrasting lithic technologies at these 'Middle Palaeolithic' sites, and demonstrated the feasibility of using pMET-pIRIR dating procedures to reassess other putative 'Middle Palaeolithic' sites in the Nihewan Basin.

Acknowledgements

This study was supported by postgraduate scholarships from the China Scholarship Council and the University of Wollongong to Y.G. (201206010053), an Australian Research Council Future Fellowship to B.L. (FT140100384), a grant from the National Natural Science Foundation of China to J.Z. (NSFC, No. 41471003), and an Australian Research Council Australian Laureate Fellowship to R.G.R. (FL130100116). We thank Weiwen Huang, Yue Hu, Yongmin Meng, Qi Wei, Shengquan Cheng, Fagang Wang, Yang Liu and others who helped with the field investigations and sample and literatures collection. The authors thank Robin Dennell and an anonymous reviewer for their constructive comments.

Appendix A. Supplementary data

Supplementary data related to this article can be found at http://dx.doi.org/10.1016/j.yqres.2016.03.002.

References

Aitken, M.J., 1985. Thermoluminescence Dating. Academic Press, London.

Aitken, M.J., 1998. An Introduction to Optical Dating. Oxford University Press, Oxford.

Ao, H., Deng, C., Dekkers, M.J., Liu, Q., 2010a. Magnetic mineral dissolution in Pleistocene fluvio-lacustrine sediments, Nihewan Basin (North China). Earth and Planetary Science Letters 292, 191–200.

Ao, H., Deng, C.L., Dekkers, M.J., Liu, Q.S., Qin, L., Xiao, G.Q., Chang, H., 2010b. Astronomical dating of the Xiantai, Donggutuo and Maliang Paleolithic sites in the Nihewan Basin (North China) and implications for early human evolution in East Asia. Palaeogeography Palaeoclimatology Palaeoecology 297, 129–137.

Blegen, N., Tryon, C.A., Faith, J.T., Peppe, D.J., Beverly, E.J., Li, B., Jacobs, Z., 2015. Distal tephras of the eastern Lake Victoria basin, equatorial East Africa: correlations, chronology and a context for early modern humans. Quaternary Science Reviews 122, 89–111.

Bøtter-Jensen, L., Mejdahl, V., 1988. Assessment of beta dose rate using a GM multicounter system. Nuclear Tracks and Radiation Measurements 14, 187–191.

Buylaert, J.P., Murray, A.S., Thomsen, K.J., Jain, M., 2009. Testing the potential of an elevated temperature IRSL signal from K-feldspar. Radiation Measurements 44, 560–565.

Chen, Y., Li, S.H., Li, B., Hao, Q., Sun, J., 2015. Maximum age limitation in luminescence dating of Chinese loess using the multiple-aliquot MET-pIRIR signals from K-feldspar. Quaternary Geochronology 30, 207–212.

David, B., Roberts, R.G., Magee, J., Mialanes, J., Turney, C., Bird, M., White, C., Fifield, L.K., Tibby, J., 2007. Sediment mixing at Nonda Rock: investigations of stratigraphic integrity at an early archaeological site in northern Australia and implications for the human colonisation of the continent. Journal of Quaternary Science 22, 449–479.

Dennell, R.W., 2013. The Nihewan Basin of North China in the Early Pleistocene: continuous and flourishing, or discontinuous, infrequent and ephemeral occupation? Quaternary International 295, 223–236.

Du, S.S., 2003. A preliminary study on raw material exploitation in Middle–Upper Palaeolithic sites in Nihewan Basin. Acta Anthropologica Sinica 22, 121–130.

Galbraith, R.F., 2005. Statistics for Fission Track Analysis. Chapman & Hall/CRC Press, Boca Raton.

Galbraith, R.F., Roberts, R.G., Laslett, G.M., Yoshida, H., Olley, J.M., 1999. Optical dating of single and multiple grains of quartz from Jinmium rock shelter, northern Australia: part I, experimental design and statistical models. Archaeometry 41, 339–364.

Galbraith, R.F., Roberts, R.G., 2012. Statistical aspects of equivalent dose and error calculation and display in OSL dating: an overview and some recommendations. Quaternary Geochronology 11, 1–27.

Gao, X., 1999. A discussion of the 'Chinese Middle Paleolithic'. Acta Anthropologica Sinica 18, 1–16 (in Chinese).

Gao, X., Norton, C.J., 2002. A critique of the Chinese 'Middle Palaeolithic'. Antiquity 76, 397–412.

Gong, Z.J., Li, S.H., Li, B., 2014. The evolution of a terrace sequence along the Manas River in the northern foreland basin of Tian Shan, China, as inferred from optical dating. Geomorphology 213, 201–212.

Guo, Y.J., Li, B., Zhang, J.F., Roberts, R.G., 2015. Luminescence-based chronologies for Palaeolithic sites in the Nihewan Basin, northern China: first tests using newly developed optical dating procedures for potassium feldspar grains. Journal of Archaeological Science: Reports 3, 31–40.

Guo, Z.T., Berger, A., Yin, Q.Z., Qin, L., 2009. Strong asymmetry of hemispheric climates during MIS-13 inferred from correlating China loess and Antarctica ice records. Climate of the Past 5, 21–31.

Han, Z.Y., Yang, C., Wang, Y., Min, L.R., 2005. Age of stromatolites at Hutouliang in Nihewan Basin. Quaternary Sciences 25, 86–92 (in Chinese with English abstract).

Huang, W.W., 2000. Stratigraphical basic of the Paleolithic sequence of China. Acta Anthropologica Sinica 19, 269–283 (in Chinese with English abstract).

Huang, W.W., Hou, Y.M., Gao, L.H., 2009. "Western Elements" in the Chinese Palaeolithic as viewed in a framework of early human cultural evolution. Acta Anthropologica Sinica 28, 16–24 (in Chinese with English abstract).

Huntley, D.J., Baril, M.R., 1997. The K content of the K-feldspars being measured in optical dating or in thermoluminescence dating. Ancient TL 15, 11–13.

Huntley, D.J., Hancock, R.G.V., 2001. The Rb contents of the K-feldspars being measured in optical dating. Ancient TL 19, 43–46.

Huntley, D.J., Godfrey-Smith, D.I., Thewalt, M.L.W., 1985. Optical dating of sediments. Nature 313, 105–107.

Huntley, D.J., Lamothe, M., 2001. Ubiquity of anomalous fading in K-feldspars and the measurement and correction for it in optical dating. Canadian Journal of Earth Sciences 38, 1093–1106.

Ikawa-Smith, F., 1978. Introduction: the early Paleolithic tradition of East Asia. In: Ikawa-Smith, F. (Ed.), Early Paleolithic in South and East Asia. Mouton, The Hague, pp. 1–10.

Jacobs, Z., Duller, G.A., Wintle, A.G., 2006. Interpretation of single grain D_e distributions and calculation of D_e. Radiation Measurements 41, 264–277.

Jacobs, Z., Wintle, A.G., Duller, G.A., Roberts, R.G., Wadley, L., 2008. New ages for the post-Howiesons Poort, late and final Middle Stone Age at Sibudu, South Africa. Journal of Archaeological Science 35, 1790–1807.

Jacobs, Z., Roberts, R.G., 2015. An improved single grain OSL chronology for the sedimentary deposits from Diepkloof Rockshelter, Western Cape, South Africa. Journal of Archaeological Science 63, 175–192.

Kleindienst, M.R., 2006. On naming things — behavioral changes in the late Middle to earlier Late Pleistocene, viewed from the eastern Sahara. In: Hovers, E., Kuhn, S.L. (Eds.), Transitions before the Transition: Evolution and Stability in the Middle Paleolithic and Middle Stone Age. Springer, New York, pp. 13–28.

Kreutzer, S., Schmidt, C., DeWitt, R., Fuchs, M., 2014. The a-value of polymineral fine grain samples measured with the post-IR IRSL protocol. Radiation Measurements 69, 18–29.

Li, B., Li, S.H., 2011. Luminescence dating of K-feldspar from sediments: a protocol without anomalous fading correction. Quaternary Geochronology 6, 468–479.

Li, B., Li, S.H., 2012. Luminescence dating of Chinese loess beyond 130 ka using the non-fading signal from K-feldspar. Quaternary Geochronology 10, 24–31.

Li, B., Li, S.H., Duller, G.A., Wintle, A.G., 2011. Infrared stimulated luminescence measurements of single grains of K-rich feldspar for isochron dating. Quaternary Geochronology 6, 71–81.

Li, B., Li, S.H., Wintle, A.G., Zhao, H., 2008. Isochron dating of sediments using luminescence of K-feldspar grains. Journal of Geophysical Research–Earth Surface 113, F02026.

Li, B., Jacobs, Z., Roberts, R.G., Li, S.H., 2013. Extending the age limit of luminescence dating using the dose-dependent sensitivity of MET-pIRIR signals from K-feldspar. Quaternary Geochronology 17, 55–67.

Li, B., Roberts, R.G., Jacobs, Z., Li, S.H., 2014a. A single-aliquot luminescence dating procedure for K-feldspar based on the dose-dependent MET-pIRIR signal sensitivity. Quaternary Geochronology 20, 51–64.

Li, B., Jacobs, Z., Roberts, R.G., Li, S.H., 2014b. Review and assessment of the potential of post-IR IRSL dating methods to circumvent the problem of anomalous fading in feldspar luminescence. Geochronometria 41, 178–201.

Li, B., Roberts, R.G., Jacobs, Z., Li, S.H., 2015a. Potential of establishing a 'global standardised growth curve' (gSGC) for optical dating of quartz from sediments. Quaternary Geochronology 27, 94–104.

Li, B., Roberts, R.G., Jacobs, Z., Li, S.H., Guo, Y.J., 2015b. Construction of a 'global standardised growth curve' (gSGC) for infrared stimulated luminescence dating of K-feldspar. Quaternary Geochronology 27, 119–130.

Li, F., 2014. Fact or fiction: the Middle Palaeolithic in China. Antiquity 88, 1303–1309.

Li, Y., Xie, F., Shi, J., 1991. Preliminary study of lithic artifacts from Banjingzi, Yangyuan, Hebei. In: IVPP (Ed.), Proceedings of the XIII International Quaternary Conference. Beijing Scientific and Technological Publishing House, Beijing, pp. 74–95 (in Chinese with English abstract).

Lian, O.B., Roberts, R.G., 2006. Dating the Quaternary: progress in luminescence dating of sediments. Quaternary Science Reviews 25, 2449–2468.

Lin, S.L., 1996. A comparison on technological modes between Chinese and western Paleolithic cultures. Acta Anthropologica Sinica 15, 1–20 (in Chinese with English abstract).

Lisiecki, L.E., Raymo, M.E., 2005. A Pliocene-Pleistocene stack of 57 globally distributed benthic $\delta^{18}O$ records. Paleoceanography 20, PA1003.

Liu, Y., Hu, Y., Wei, Q., 2013. Early to Late Pleistocene human settlements and the evolution of lithic technology in the Nihewan Basin, North China: a macroscopic perspective. Quaternary International 295, 204–214.

Meng, Y.M., Zhang, J.F., Qiu, W.L., Fu, X., Guo, Y.J., Zhou, L.P., 2015. Optical dating of the Yellow River terraces in the Mengjin area (China): first results. Quaternary Geochronology 30, 219–225.

Monnier, G., 2006. The Lower/Middle Paleolithic periodization in Western Europe. Current Anthropology 47, 709–744.

Movius, H.L., 1948. The Lower Palaeolithic cultures of southern and eastern Asia. Transactions of the American Philosophical Society 38, 329–420.

Mu, H.S., Xu, Q.H., Zhang, S.R., Hun, L.Y., Li, M.Y., Li, Y., Hu, Y.N., Xie, F., 2015. Pollen-based quantitative reconstruction of the paleoclimate during the formation process of Houjiayao Relic Site in Nihewan Basin of China. Quaternary International 374, 76–84.

Nian, X.M., Gao, X., Xie, F., Mei, H.J., Zhou, L.P., 2014. Chronology of the Youfang site and its implications for the emergence of microblade technology in North China. Quaternary International 347, 113–121.

Nian, X.M., Zhou, L.P., Yuan, B.Y., 2013. Optical stimulated luminescence dating of terrestrial sediments in the Nihewan Basin and its implication for the evolution of ancient Nihewan Lake. Quaternary Sciences 33, 403–414.

Norton, C.J., Gao, X., Feng, X.W., 2009. The East Asian Middle Palaeolithic reexamined. In: Camps, M., Chauhan, P. (Eds.), Sourcebook of Paleolithic Transition. Springer, Dordrecht, pp. 245–254.

Olley, J.M., Caitcheon, G.G., Roberts, R.G., 1999. The origin of dose distributions in fluvial sediments, and the prospect of dating single grains from fluvial deposits using optically stimulated luminescence. Radiation Measurements 30, 207–217.

Olley, J.M., Pietsch, T., Roberts, R.G., 2004. Optical dating of Holocene sediments from a variety of geomorphic settings using single grains of quartz. Geomorphology 60, 337–358.

Prescott, J.R., Hutton, J.T., 1994. Cosmic ray contributions to dose rates for luminescence and ESR dating: large depths and long-term time variations. Radiation Measurements 23, 497–500.

Roberts, R.G., Lian, O.B., 2015. Illuminating the past. Nature 520, 438–439.

Roberts, R.G., Galbraith, R.F., Yoshida, H., Laslett, G.M., Olley, J.M., 2000. Distinguishing dose populations in sediment mixtures: a test of single-grain optical dating procedures using mixtures of laboratory-dosed quartz. Radiation Measurements 32, 459–465.

Roberts, R.G., Jacobs, Z., Li, B., Jankowski, N.R., Cunningham, A.C., Rosenfeld, A.B., 2015. Optical dating in archaeology: thirty years in retrospect and grand challenges for the future. Journal of Archaeological Science 56, 41–60.

https://doi.org/10.1016/j.yqres.2016.03.002 Published online by Cambridge University Press

Thomsen, K.J., Murray, A.S., Jain, M., Bøtter-Jensen, L., 2008. Laboratory fading rates of various luminescence signals from feldspar-rich sediment extracts. Radiation Measurements 43, 1474–1486.
Tong, H.W., 2012. New remains of *Mammuthus trogontherii* from the early Pleistocene Nihewan beds at Shanshenmiaozui, Hebei. Quaternary International 255, 217–230.
Wang, H.Q., Deng, C.L., Zhu, R.X., Xie, F., 2006. Paleomagnetic dating of the Cenjiawan Paleolithic site in the Nihewan Basin, northern China. Science in China (Series D) 49, 295–303.
Wei, Q., 1997. The framework of archaeological geology of the Nihewan basin. In: Tong, Y.S. (Ed.), Evidence of Evolution — Essays in Honor of Prof. Chungchien Young on the Hundredth Anniversary of His Birth. China Ocean Press, Beijing, pp. 193–207 (in Chinese with English abstract).
Wintle, A.G., 1973. Anomalous fading of thermoluminescence in mineral samples. Nature 245, 143–144.
Wintle, A.G., 2014. Luminescence dating methods. In: Holland, H., Turekian, K. (Eds.), Treatise on Geochemistry, second ed., vol. 14. Elsevier, Oxford, pp. 17–35.
Xia, Z.K., Han, J.Q., 1998. Ecological environment of lacustrine stromatolites in the Hutouliang, Nihewan Basin. Quaternary Sciences 4, 344–350.
Xie, F., Li, J., Liu, L.Q., 2006. Paleolithic Archeology in the Nihewan Basin. Huashan Literature and Arts Press, Shijiazhuang (in Chinese).
Xie, F., Mei, H.J., Wang, Y.P., 1996. The excavation of the Que-er-gou site in the Nihewan Basin. Wenwu Jikan 4, 3–9 (in Chinese with English abstract).
Yang, Q., Chen, T.M., Hu, Y.Q., Xia, Z.K., 1993. ESR and U-series dating of stromatolite samples from Nihewan basin. Nuclear Techniques 16, 217–220.
Yee, M.K., 2012. The Middle Palaeolithic in China: a review of current interpretations. Antiquity 86, 619–626.
Yuan, B.Y., Zhu, R.X., Tian, W.L., Cui, J.X., Li, R.Q., Wang, Q., Yan, F.H., 1996. Magnetostratigraphic dating on the Nihewan Formation. Science in China (Series D) 26, 67–73 (in Chinese).
Yuan, B.Y., Tong, H.W., Wen, R.L., Wang, Y.H., 2009. The formation mechanism of the Nihewan paleo-lake and its relationship with living environment for early ancient human. Journal of Geomechanics 15, 77–87 (in Chinese with English abstract).
Yuan, B.Y., Xia, Z.K., Niu, P.S. (Eds.), 2011. Nihewan Rift and Early Man. Geology Press, Beijing (in Chinese).
Zhao, H., Li, S.H., 2005. Internal dose rate to K-feldspar grains from radioactive elements other than potassium. Radiation Measurements 40, 84–93.
Zhao, H., Lu, Y., Wang, C., Chen, J., Liu, J., Mao, H., 2010. ReOSL dating and fluvial sediments from Nihewan Basin, northern China and its environmental application. Quaternary Geochronology 5, 159–163.
Zhu, R.X., Hoffman, K.A., Potts, R., Deng, C.L., Pan, Y.X., Guo, B., Shi, C.D., Guo, Z.T., Yuan, B.Y., Hou, Y.M., Huang, W.W., 2001. Earliest presence of humans in northeast Asia. Nature 413, 413–417.
Zhu, R.X., Potts, R., Xie, F., Hoffman, K.A., Deng, C.L., Shi, C.D., Pan, Y.X., Wang, H.Q., Shi, R.P., Wang, Y.C., Shi, G.H., Wu, N.Q., 2004. New evidence on the earliest human presence at high northern latitudes in northeast Asia. Nature 431, 559–562.
Zhu, R.X., Deng, C.L., Pan, Y.X., 2007. Magnetochronology of the fluvio-lacustrine sequences in the Nihewan Basin and implications for early human colonization of northeast Asia. Quaternary Sciences 27, 922–944 (in Chinese with English abstract).
Zhang, J.F., Zhou, L.P., 2007. Optimization of the 'double SAR' procedure for polymineral fine grains. Radiation Measurements 42, 1475–1482.

https://doi.org/10.1016/j.yqres.2016.03.002 Published online by Cambridge University Press